Basis for the phototaxis sign reversal in the green alga *Chlamydomonas reinhardtii* studied by high-speed observation

Masako Nakajima[1,2†] Kosuke Iizuka[3†], Noriko Ueki[4], Atsuko Isu[1], Kenjiro Yoshimura[5], Toshiyuki Nakagaki[3], Toru Hisabori[1,2,6], Katsuhiko Sato[3*], and Ken-ichi Wakabayashi[1,2,6*]

1: Laboratory for Chemistry and Life Science, Institute of Innovative Research, Tokyo Institute of Technology, Yokohama, 226-8503 Japan

2: Department of Environmental Chemistry and Engineering, Interdisciplinary Graduate School of Science and Engineering, Tokyo Institute of Technology, Yokohama, 226-8503 Japan

3: Research Institute for Electronic Science (RIES), Hokkaido University, Sapporo 001-0020, Japan

4: Science Research Center, Hosei University, 2-17-1 Fujimi, Chiyoda-ku, Tokyo 102-8160, JAPAN

5: Department of Machinery and Control Systems, College of Systems Engineering and Science, Shibaura Institute of Technology, Saitama 337-8570, Japan

6: School of Life Science and Technology, Tokyo Institute of Technology, Yokohama, 226-8503 Japan

†: These authors contributed equally to this work.

*: To whom correspondence should be addressed: KW, wakaba@res.titech.ac.jp; KS, katsuhiko_sato@es.hokudai.ac.jp

ABSTRACT

For organisms that respond to environmental stimuli using taxes, reversal of the tactic sign should be tightly regulated for survival. The biciliate green alga *Chlamydomonas reinhardtii* is an excellent model for studying reversal between positive and negative phototaxis. *C. reinhardtii* cells change swimming direction by modulating the balance of beating forces between their two cilia after photoreception at the eyespot; however, it remains unknown how they reverse phototactic sign. In this study, we observed cells undergoing phototactic turns with a high-speed camera and found that two key factors determine the phototactic sign: which of the two cilia beats stronger for phototactic turning and when the strong beating starts. We developed a mathematical model to explain this sign-reversal with a single equation, which suggests that the timing of the strong ciliary beating is regulated by switching between the light-on and light-off responses at the eyespot.

Keywords:

Chlamydomonas reinhardtii, phototaxis, flagella/cilia, ROS, mathematical model

INTRODUCTION

The biciliate unicellular green alga *Chlamydomonas reinhardtii* is an excellent model organism to study how organisms respond to changing light conditions. *C. reinhardtii* shows a distinct light-induced behavior known as phototaxis, in which cells swim either toward or away from a light source (in positive or negative phototaxis, respectively). The direction of phototaxis, referred to here as the sign (either positive or negative), can be switched. The regulation of this sign reversal is thought to be important for the viability of photosynthetic algae, but its mechanism is not well understood.

In *C. reinhardtii*, the light signal for phototaxis is received by the eyespot (Foster & Smyth, 1980), an organelle that appears under a microscope as an orange spot near the cell equator. It consists of carotenoid-rich granule layers, and a small area of plasma membrane in which channelrhodopsin (ChR) molecules are localized (Fig. 1A). The carotenoid-rich granule layers (CLs) function as a quarter-wave plate that reflects light (Foster & Smyth, 1980; Ueki et al., 2016), while ChR molecules are light-gated ion channels (Nagel et al., 2002; Nagel et al., 2003; Oleg A. Sineshchekov, Jung, & Spudich, 2002; Suzuki et al., 2003). Because of the relative position of these two components, the eyespot perceives light with high directionality. When a light signal arrives from the ChR-facing side, the light signal is amplified by reflection from the

CLs; conversely, light signals are blocked by the CLs when coming from the CL-facing direction. In addition, while swimming, the cell rotates around its anterior-posterior axis. Directional photoreception by cells that swim with bodily rotation enables them to accurately detect and move in the direction of light stimuli.

Previous studies suggest that the phototaxis pathway in *C. reinhardtii* consists of: 1) photoreception by ChRs, 2) an increase in intraciliary [Ca^{2+}], and 3) a change in the balance of beating between the two cilia – after photoreception, the forces generated by the two cilia of *C. reinhardtii* become imbalanced, changing the cell's swimming direction. These two cilia can be distinguished by their position relative to the eyespot, with the one nearest the eyespot called the *cis*-cilium, and the other called the *trans*-cilium. A currently prevailing model explains the mechanism underlying positive phototaxis as follows: When the eyespot faces a light source during swimming with bodily rotation, ChRs open to allow for Ca^{2+} entry, intraciliary [Ca^{2+}] increases, and the *trans*-cilium starts to beat more strongly than the *cis*-cilium, by increasing beating amplitude and/or frequency (Ritsu Kamiya & Witman, 1984; Rüffer & Nultsch, 1991). The imbalance between the forces generated by the two cilia tilts the cell's swimming direction toward the eyespot-bearing side (i.e., in the direction of the light source). After 180° of rotation, the eyespot stops receiving light due to the shielding of CLs, the ChRs

close, intraciliary [Ca^{2+}] decreases due to some ion pumping activity, and the force generated by the *cis*-cilium increases while that of the *trans*-cilium decreases, resulting in the cell's swimming direction tilting toward the light-source. By repeating this process, the cell will swim toward the light source, displaying positive phototaxis (Fig. 1B). However, in contrast to this widespread model, phototactic turns may also be initiated when the eyespot faces away from the light source (i.e., when the eyespot is shaded) (Isogai, Kamiya, & Yoshimura, 2000).

How, then, can the direction of phototaxis be reversed? The following possibilities exist: (i) The *cis*-cilium, rather than the *trans*-cilium, beats stronger when $[Ca^{2+}]_i$ increases upon photoreception; (ii) A light-off stimulus on the eyespot, rather than a light-on stimulus, activates the dominant *trans*-cilium; (iii) The response of cilia to a light-on stimulus on the eyespot is delayed; or (iv) $[Ca^{2+}]_i$ actually decreases upon photoreception, rather than increasing. Among these possibilities, (iv) must be tested using highly sensitive Ca^{2+} indicators, because the $[Ca^{2+}]_i$ regulating the beating of cilia during phototaxis is thought to be at submicromolar levels (Ritsu Kamiya & Witman, 1984), while (i) to (iii) can be tested by observing cell behavior after light stimulation.

Indeed, several factors are known to induce sign-switching of phototaxis in *C. reinhardtii*, including both extracellular factors like light intensity (Feinleib & Curry,

96 1971) and extracellular Ca^{2+} concentration (Morel-Laurens, 1987), and intracellular
97 factors such as circadian rhythms (Kondo, Johnson, & Hastings, 1991), photosynthetic
98 activities (Takahashi & Watanabe, 1993), and the amount of reactive oxygen species
99 (ROS) (Wakabayashi, Misawa, Mochiji, & Kamiya, 2011). The amount of cellular ROS
100 can be readily changed by applying membrane-permeable ROS reagents or
101 membrane-permeable ROS scavengers to cells, which strongly bias the phototactic sign:
102 cells show positive phototaxis after treatment with ROS and negative phototaxis after
103 treatment with ROS-scavengers (Wakabayashi et al., 2011).
104 In this study, to test the possibilities (i) to (iii) above, we carried out
105 high-speed observations of cells turning during positive or negative phototaxis, after
106 treatment with either a membrane-permeable ROS or a membrane-permeable ROS
107 scavenger (hereinafter referred to as “ROS-modulating reagents”). Our results support
108 both possibilities (i) and (ii) described above. In support of (i), after photoreception, we
109 observed that positively phototactic cells beat the *trans*-cilium more strongly, whereas
110 negatively phototactic cells beat the *cis*-cilium more strongly. We also developed a
111 mathematical model that can explain the phototactic-sign reversal based on the change
112 in timing at which ciliary dominance takes place after photo-stimulation. In support of
113 (ii), treatment with the ROS-modulating reagents was found to induce a light-off

response, which switched the phototactic sign. While it was impossible to distinguish between possibilities (ii) (light-off response) and (iii) (delay of light-on response) through microscopic observation of the wild-type cells alone, our observations of slow-swimming mutants, along with the results of our mathematical model, strongly support possibility (ii).

RESULTS

Two hypotheses to explain the sign change of phototaxis

The mechanism underlying positive phototaxis can be explained as described in the Introduction (shown in Fig. 1B). To elucidate the mechanism of negative phototaxis, we considered two models (Fig. 1C), in which the dominant cilium is a key factor (defined here as the cilium that begins to beat more strongly after photoreception than the other). In the first model (the dominant-arm model), we assume that the relationship between the dominant cilium and $[Ca^{2+}]_i$ is reversed, such that the *cis*-cilium, rather than the *trans*-cilium, becomes dominant when $[Ca^{2+}]_i$ is increased. If the *cis*-cilium beats more strongly than the *trans*-cilium after light perception (which elicits Ca^{2+} influx), the cell will undergo negative phototaxis. In the second model (the off-response model), we assume that the relationship between the dominant cilium and $[Ca^{2+}]_i$ remains the same, but the onset of ciliary dominance (along with $[Ca^{2+}]_i$ increase) occurs when the eyespot faces away from the light source, and senses a light-off stimulus. In this case, the cell will also show negative phototaxis.

Dominant cilia differ in strains with opposite phototactic signs

137 To determine which of these two models was more plausible, we observed the turning
138 of *C. reinhardtii* cells using a high-speed camera (150 fps) linked to green
139 light-emitting diode (LED) illumination sources at right angles. This system was an
140 extension of the right-angle illumination system originally designed for the previous
141 study (Isogai et al., 2000), which we here improved upon to observe the phototactic
142 turnings and the eyespot position simultaneously by synchronizing the high-speed
143 camera and the LED illumination. This allowed us to determine the exact time when a
144 light stimulus was applied to a rotating cell, and the simultaneous orientation of the
145 eyespot (visible as a bright spot under a dark-field microscope with an oil-immersion
146 condenser). With this system, we first induced phototaxis in cells using the weaker
147 stimulus of Light 1 (Fig. 2A). Then, the stronger Light 2 was illuminated at right angles
148 to Light 1. When the eyespot in a swimming cell faced the light-source side of Light 2
149 (or the light side) after its illumination, we considered the cell to have perceived the
150 light in that time frame (Fig. 2A). Then, from the position of the eyespot and the
151 swimming path, we assessed which cilium beat more strongly.

152 We observed the eyespot position during phototactic turning in two genetically
153 different strains, CC-124 (a negatively phototactic strain, here referred to as NP) and
154 CC-125 (positively phototactic strain, PP) (see Materials and Methods). We analyzed

155 only those cells that showed phototactic turnings of one full self-rotation after
156 photoreception. We found that PP cells usually showed positive phototaxis. Similar to
157 the PP cell after treatment with *t*-BOOH that induces positive phototaxis in Fig. 2A, a
158 typical control PP cell changed its swimming direction immediately after it detected
159 Light 2 (green arrow position). When turning toward the direction of the light source,
160 more than half of the cells performed phototactic turning while the eyespot was located
161 on the light side (i.e., the *trans*-cilium became dominant immediately after
162 photoreception) (Fig. 2B).

163 In contrast, NP cells usually showed negative phototaxis. Similar to the NP cell
164 after treatment with DMTU that induces negative phototaxis in Fig. 2A, a typical
165 control NP cell changed its swimming direction immediately after it detected Light 2,
166 similar to the PP cell. When turning against the direction of the light source, most cells
167 performed turns while the eyespot was located on the light side, i.e. the *cis*-cilium
168 became dominant immediately after photoreception (Fig. 2B). These observations
169 suggest that the difference between PP and NP cells can be explained by the "Dominant
170 arm model." The cilium that becomes dominant after photoreception is genetically
171 determined. Therefore, if the dominant cilium is the *trans*-cilium, the strain tends to

show positive phototaxis, while if it is the *cis*-cilium in another strain, it tends to show negative phototaxis.

Reversal of phototactic sign by "off-response" of the dominant cilium

Next, we examined the effect of reagents that change the cellular ROS, affecting the phototactic sign. After treatment with 0.2 mM *t*-BOOH, a membrane-permeable ROS reagent that induces positive phototaxis in both strains, most PP cells made phototactic turns while the eyespot was located on the light side, while most NP cells made phototactic turns while the eyespot was located on the dark side (i.e., the side opposite the light-source) (Fig. 2B). Fig. 2A shows the representative data, and the *t*-BOOH-treated NP cell changed its swimming direction after the cell made a half-self-rotation (magenta arrow). In contrast, after treatment with 75 mM DMTU, a membrane-permeable ROS scavenger that induces negative phototaxis in both strains, most PP cells made phototactic turns while the eyespot was located on the dark side, and most NP cells made phototactic turns while the eyespot was located on the light side. In Fig. 2A, the DMTU-treated PP cell changed its swimming direction after the cell made a half-self-rotation (magenta arrow).

Thus, the sign-reversal of phototaxis in both strains can be explained by the off-response model; i.e., *t*-BOOH induces the onset of *cis*-cilium dominance in the dark side in NP cells and DMTU induces that of *trans*-cilium dominance in the light side in PP cells. Simply put, the reversal of genetically determined phototactic signs in a given strain is achieved by reversing the eyespot position relative to the light source (the light or dark side) when its genetically determined dominant cilium starts to show stronger beating than the other after light stimulation. We found that the dominant cilium after photoreception of PP cells was always the *trans*-cilium, while that of NP was always the *cis*-cilium. In each strain, the sign-switching of phototaxis was caused by the onset of strong beating of the dominant cilium on the dark side.

Therefore, these phototactic turning events can be categorized into two cases for each sign of phototaxis. For cells displaying positive phototaxis: in (Positive Case 1), phototactic turning occurred while the eyespot was located on the light side. In this case, the *trans*-cilium must have become dominant in response to the light-on stimulus (such as PP cells without the ROS-reagents or with *t*-BOOH). In (Positive Case 2), phototactic turning occurred while the eyespot was located on the dark side. In this case, the *cis*-cilium must have become dominant in response to the light-off stimulus (such as NP cells with *t*-BOOH). For cells displaying negative phototaxis: in (Negative Case 1),

phototactic turning occurred while the eyespot was located on the light side. In this case, the *cis*-cilium must have become dominant in response to the light-on stimulus (such as NP cells without the ROS-reagents or with DMTU). In (Negative Case 2), phototactic turning occurred while the eyespot was located on the dark side. In this case, the *trans*-cilium must have become dominant in response to the light-off stimulus (such as PP cells with DMTU).

Eyespot position in the helical paths

Regarding changes in the balance of beating between the two cilia during phototactic turning, we first wanted to examine the force balance in unstimulated cells. Under homogeneous light conditions, *C. reinhardtii* cells swim in a helical path, due to the imbalanced force generation of the two cilia beating in slightly skewed planes (Fig. S1A). In previous work, Isogai et al. showed that the eyespot is located on the outer edge of the helical swimming paths in ~80 percent of positively phototactic cells (Isogai et al., 2000). In contrast, for negatively phototactic cells, ~50 percent of cells swim with the eyespot facing inside, whereas ~30 percent of cells swim with the eyespot facing outside (Isogai et al., 2000). These results suggest that eyespot position in the helical swimming path is partially correlated with the phototactic sign, but the correlation is not

225 determinative. We thus investigated whether the eyespot position in the swimming
226 paths is affected by ROS-modulating reagents. Most, but not all, cells swam with the
227 eyespot outside the helix when they showed either positive phototaxis (Fig. S1B, Sign
228 P). However, when cells showed negative phototaxis in the presence of DMTU,
229 directing the eyespot inside the helix was observed almost as frequently as towards the
230 outside (Fig. S1B, Sign N, +DMTU). Thus, we did not observe a strict correlation either
231 between phototactic sign and eyespot position in the helical paths.
232
233 **Photoreceptor currents after treatment with the ROS-modulating reagents**
234 A possible explanation for how ROS-modulating reagents induce the light-off response
235 is that those reagents delay the response of the dominant cilium by slowing the opening
236 of photo-gated channels (ChRs). If this delay is as long as the time required for a cell to
237 perform a half rotation (~250 msec), then the phototactic sign of the cell would reverse.
238 To test this possibility, we measured the photoreceptor current (PRC) in a population of
239 *C. reinhardtii* cells by the method of Sineshchekov et al. (O. A. Sineshchekov,
240 Govorunova, Der, Keszthelyi, & Nultsch, 1992, 1994) (Fig. S2A). Treatment with
241 *t*-BOOH did not significantly affect the magnitude of PRC produced by a single flash of
242 light stimulation, in either PP or NP cells (Fig. S2B, C). We also measured the time

243 (delay) required for the generation of PRC after photostimulation, but detected no
244 significant difference between the control and the *t*-BOOH-treated cells (Fig. S2B, C).
245 In contrast, after treatment with DMTU, we found that PRC decreased, while delay time
246 increased, in both strains (Fig. S2B, C). However, the increase in delay time was only
247 ~1 msec. These results suggest that the light-off response is not caused by the delay in
248 PRC generation.
249

250 **Mathematical model to test the experimental data**

251 Our experimental results suggest that two factors are important for reversal of the
252 phototactic sign in *C. reinhardtii* cells: (1) which of the two cilia becomes dominant
253 after photoreception, and (2) when such a change in dominance takes place. To
254 quantitatively examine these factors, we developed a simple mathematical model that
255 describes the swimming behaviors of *C. reinhardtii*, focusing on the timing of the
256 appearance of ciliary dominance. We also considered whether the ciliary dominance
257 taking place on the dark side might either be caused by the light-off stimulus, or result
258 from a delay in the light-on response with this model.

259 Our modeling framework is based on previous models of phototaxis in *C.*
260 *reinhardtii* and the multicellular green alga *Volvox carteri* (Bennett & Golestanian,

2015; Drescher, Goldstein, & Tuval, 2010), which we extend by explicitly introducing a time delay into the ciliary response after a light stimulus (see SI Appendix A for details). We approximate the cell as a rigid ball and define the body axes of the cell as in Fig. 3A, where **a, b** and **c** are unit vectors that are fixed to the body of the cell. We assume that a cell swims with cilia forward, with a constant speed v_0 in the posterior direction **c**, i.e., $\mathbf{v} = v_0\mathbf{c}$, and rotates with the angular velocity

$$\boldsymbol{\omega}(t) = -\omega_c^{(0)}\,\mathbf{c} + (\omega_a^{(0)} - p(t))\mathbf{a}\,, \quad --[1]$$

where $\omega_c^{(0)}$ and $\omega_a^{(0)}$ are constants. p expresses the contribution from the change in the behaviors of the two cilia: when the *trans*-cilium beats stronger than the *cis*-cilium, p becomes positive, and vice versa. The data in Fig. 2 indicate that the beating balance between the two cilia changes depending on the change in the light intensity received at the eyespot, I, with some delay time. We thus relate p and I as

$$p(t) = \gamma_0 \frac{dI(t-\tau_0)}{dt}, \quad --[2]$$

where γ_0 is a constant that takes the value +1 or -1. $\gamma_0 = +1$ means the *trans*-cilium is dominant (as in PP), while $\gamma_0 = -1$ means the *cis*-cilium is dominant (as in NP). τ_0 is the delay time of the onset of the ciliary dominance after photoreception (around 30-40 msec under normal culture conditions) (Rüffer & Nultsch, 1991; Witman, 1993). We consider the situation where a parallel light comes from the positive z direction (Fig. 3B), and I is given by $I(t) = I_0(-\mathbf{e}_{light}\cdot\mathbf{e}_{eyespot} + 1)/2$, where $\mathbf{e}_{light} = (0,0,-1)$, $\mathbf{e}_{eyespot} = (\mathbf{a}+\mathbf{b})/\sqrt{2}$ and I_0 is the intensity of the light; $\mathbf{e}_{light}$ and $\mathbf{e}_{eyespot}$ represent the

direction of the incident light and the eyespot, respectively. The directions of body axes, **a**, **b**, **c**, are specified by three variables, the Euler angles $(\theta_1, \theta_2, \theta_3)$ (Fig. 3B) (Landau, 1976). This model is described by the variables $(\theta_1, \theta_2, \theta_3)$ and the position of the cell $\mathbf{r} = (x, y, z)$ (see Appendix A), and their time evolution equations are closed in terms of the variables.

The model has two characteristic steady solutions (Eqs. S5 and S6): one represents positive phototaxis, where the cell swims in the positive z direction with a constant speed, drawing a right-handed spiral trajectory. The other represents negative phototaxis, where the cell swims in the opposite direction in a similar way (Fig. 3D). Thus the model intrinsically accounts for both positive and negative phototaxis states. The stability of the two states changes with the parameters involved in the relation between p and I, (i.e., γ_0, I_0 and τ_0). To examine how these parameters determine the steady state (i.e., the final swimming direction), we conducted numerical simulations with appropriate initial conditions of $(\theta_1, \theta_2, \theta_3, \mathbf{r})$. The results showed that a cell with the *trans*-flagellum dominant (γ_0 =+1) shows positive phototaxis when τ_0 =0.08 sec, and negative phototaxis when τ_0 =0.32 sec (Fig. 3C, D). As one full rotation of the cell about **c** axis takes 0.5 sec in this simulation ($\omega_c^{(0)} = 4\pi$), a τ_0 value between 0 and 0.25 means that the onset of ciliary dominance occurrs on the light side (when the eyespot faces the light source), whereas τ_0 between 0.25 and 0.50 means that it occurrs on the dark side (when the eyespot faces opposite the light source after photostimiulation). Thus, the simulation results are consistent with our experimental results of the PP strain (Fig. 2).

Fig. 4 shows the average velocities in the z direction (parallel to the light axis) in the steady state for various values of γ_0, I_0 and τ_0. Blue dots are the states where Eq. S5 (positive phototaxis) is realized, while red dots are the states in which Eq. S6 (negative phototaxis) is realized. Black dots represent states other than Eqs. S5 and S6, in which the cell does not draw a simple spiral trajectory but a complex one (Fig. S3), where $v(t)$ oscillates. The following three properties of our model are apparent from Fig. 4: (i) When the sign of γ_0 (representing the dominant cilium) is changed, the sign of $\bar{v}_z$ (representing the phototactic sign) changes. (ii) When τ_0 (the delay time of the onset of ciliary dominance after photoreception) changes, the sign of $\bar{v}_z$ also changes. (iii) When I_0 (the maximum light intensity that the cell senses) increases, the blue and red dot regions decrease and the black dot regions increase. Property (i) validates the Dominant-arm model (Fig. 1C), which agrees with the previous mathematical model (Bennett & Golestanian, 2015). Property (ii) validates the Off-response model (Fig. 1C) as long as $0.25<\tau_0<0.5$, a range that is consistent with the present study. Property (iii) indicates that the increase in I_0 destabilizes Eqs. S5 and S6 (see SI Appendix B and Fig. S3 for details), implying that intense light tends to make the movement of *C. reinhardtti* unstable.

Off-response or delayed response?

In the Off-response model, ciliary dominance starts to occur on the dark side. We interpreted this as an immediate response to a light-off signal. However, it may also be a

delayed response to a light-on signal. If the delay time τ_0 is fixed between 0.25 sec and 0.5 sec, a delayed response to a light-on stimulus would just look like a light-off response without a delay. To assess which of these two interpretations is more plausible, we conducted an experiment and a simulation.

First, we observed phototaxis in slow-swimming mutants *ida4* (lacking inner-arm dynein subspecies a, c and d) and *oda1* (lacking entire outer-arm dynein) after treatment with ROS-modulating reagents (R. Kamiya, 1988; R. Kamiya, Kurimoto, & Muto, 1991; Takada, Wilkerson, Wakabayashi, Kamiya, & Witman, 2002). As the bodily rotation of the cell is caused by the slightly three-dimensional beating of the two cilia, slow-swimming mutants show bodily rotation with a longer rotation cycle time, as we observed (Table 1). If the delay time is between 0.25 and 0.50 sec, those slow-swimming mutants may differ in phototactic sign from the wild-type PP and NP strains. We found that both *oda1* and *ida4* cells tended to display positive phototaxis under neutral or oxidizing conditions, and negative phototaxis under reducing conditions, similarly to the PP strain of the wild type (Fig. 5). However, the sign-reversal in the slow-swimming mutants was not as clear as in the wild type, especially after treatment with the ROS-scavenger. It is possible that the force generation for steering is weaker under these conditions in the slow-swimming mutants.

We also used our mathematical model to simulate the behavior of cells that self-rotate at a lower-than-normal frequency of 0.67 Hz, a frequency close to that of *oda1* (0.72 Hz; Table 1). Our simulation results indicated that when τ_0 is between 0.25 and 0.5 sec, such cells do not change phototactic signs with a change in τ_0, unlike the wild type cells that rotate at higher frequencies of ~2 Hz (Fig. 6). Taken together, these results suggest that, in the slow-swimming mutants (and most likely in the PP and NP strains also), it is more likely that the onset of ciliary dominance alteration on the dark side takes place in direct response to a light-off stimulus, rather than as a delayed response to a light-on stimulus.

DISCUSSION

In this study, we observed phototactic turning of *C. reinhardtii* cells with high-speed video recording. As previously shown (Wakabayashi et al., 2011), both PP and NP cells changed the sign of phototaxis when treated with ROS-modulating agents. Our results demonstrate that the sign of phototaxis is determined by which of the two (*cis*- and *trans*-) cilia beats stronger after photoreception, and that the sign reverses depending on whether the dominant cilium begins to beat stronger when the eyespot faces the light source or away from it (Fig. 7). An important factor that modulates when the onset of ciliary dominance occurs is the intracellular amount of ROS. Our mathematical model supports these findings.

The cilium that becomes dominant after photoreception

The first key factor that determines the phototactic sign is whether the *cis*- or the *trans*-cilium is dominant in a given strain. Several previous studies have shown that the two cilia of *C. reinhardtii* are intrinsically different (R. Kamiya & Hasegawa, 1987; Ritsu Kamiya & Witman, 1984; Ruffer & Nultsch, 1987, 1998; Rüffer & Nultsch, 1991). Rüffer and Nultsch (1991, 1998) carried out high-speed cinematographic observation on cells trapped with a suction pipette. They found that, upon

370 photo-stimulation, the *trans*-cilium tended to beat more strongly (with a larger
371 amplitude and at a higher frequency) than the other in positively phototactic strains,
372 whereas the *cis*-cilium beat more strongly than the other in negatively phototactic
373 strains (Ruffer & Nultsch, 1998; Rüffer & Nultsch, 1991). Our results, obtained from
374 observation of free-swimming cells undergoing phototactic turning, are consistent with
375 these studies.

376 How is the dominant cilium determined? The results of the present study, as
377 well as those of Rüffer and Nultsch (1991), indicate that the cilium that becomes
378 dominant after photostimulation is the *trans*-cilium in PP and the *cis*-cilium in NP cells.
379 One would be inclined to assume that the Ca^{2+} sensitivities of the *cis*- and
380 *trans*-axonemes (the inner structure of cilia) are reversed between PP and NP. However,
381 in detergent-extracted and motility-reactivated cell models, the Ca^{2+}-dependent motility
382 of the two axonemes attached to a single cell body was found not to differ between PP
383 and NP strains (Wakabayashi et al., 2011). Therefore, factors other than axonemes may
384 cause differences in ciliary Ca^{2+}-response of PP and NP cells. For example, some
385 detergent-soluble constituents of cilia, or some chemical modification of the axoneme
386 that is not retained after detergent extraction, may be responsible.

Previously, we identified the defect that causes the negatively phototactic phenotype in the NP strain (*agg1*) as the loss of a protein that possibly functions in mitochondria (Ide et al., 2016). If this protein functions in the respiratory chain, the redox poise and/or the amount of ROS could differ between PP and NP cells and differentially modulate the activities of membrane proteins, such as Ca^{2+} channels and pumps. Other *C. reinhardtii* mutants, *agg2* and *agg3*, are also known to display negative phototaxis. Although whether the *cis*- or the *trans*-cilium is dominant in these mutants has not been determined, their defects are also caused by mutations in non-axonemal proteins; the causative protein Agg2 is localized to the proximal ciliary membrane, while Agg3 is a flavodoxin that localizes to the ciliary matrix (Iomini, Li, Mo, Dutcher, & Piperno, 2006). Loss of these proteins may modulate the function of the ciliary membrane and could switch the dominant cilium.

How is the off-response of the ciliary dominance produced?

The second key factor that determines the phototactic sign is the timing at which the dominant cilium starts to increase power after photoreception. We showed that *t*-BOOH, a membrane-permeable ROS that promotes positive phototaxis, induces the onset of *cis*-cilium dominance on the dark side in NP cells, whereas DMTU, a

405 membrane-permeable ROS-scavenger that promotes negative phototaxis, induces that of
406 the *trans*-cilium dominance on the dark side in PP cells (Fig. 2A, B). The onset of
407 ciliary dominance on the dark side could be interpreted as a so-called off response or a
408 step-down response, which means that cells respond to a light-off stimulus. Initiation of
409 phototactic turn as an off response has been proposed previously (Isogai et al., 2000),
410 and the present study provides evidence for this from simultaneous observation of
411 swimming track and eyespot position while artificially manipulating the phototaxis
412 direction. Rüffer and Nultsch (1991) showed that the beating in the two cilia
413 reciprocally changes upon reception of light-on as well as light-off stimuli, and
414 suggested that cells displaying opposite cilia responses exhibit positive and negative
415 phototaxis, which our results are in general agreement with.

416 The molecular mechanism of the off response in *C. reinhardtii* is unknown.
417 Theoretically, a response equivalent to an off-response could be accomplished by an
418 appropriate delay in the light-on response. However, our observations on
419 slow-swimming mutants, as well as theoretical considerations, rule out this possibility.
420 Previous observations by Rüffer and Nultsch (1991) that micropipette-held *C.*
421 *reinhardtii* cells display on- and off- responses also indicate the presence of a genuine
422 off-response. Generally, the photoreception by ChR, a light-gated cation channel, is

423 thought to induce depolarization of the cellular membrane. However, the Ca^{2+} influx at
424 the eyespot may induce activation of Ca^{2+}-activated K^+ channel (Vergara, Latorre,
425 Marrion, & Adelman, 1998), which would induce an increase in K^+ conductance and
426 concomitant hyperpolarization of the membrane. If the light causes hyperpolarization, a
427 light-off stimulus may induce depolarization of the membrane and elicit an off-response.
428 In addition, recently, ROS-modulating reagents were shown to modulate the
429 phosphorylation state of ChR1 (Bohm et al., 2019). The activity change of ChR1
430 according to this phosphorylation state may also lead to the off-response. These
431 possibilities can be tested by further electrophysiological analyses using
432 ROS-modulating reagents.
433
434 **Mathematical model results support the experimental data**
435 To mathematically assess the plausibility of the Dominant arm model and the
436 Off-response model, we developed a simple model that describes the swimming
437 behaviors of *C. reinhardtii*. The theoretical model and the experimental data both
438 showed that the Off-response model is not accomplished by the presence of a fixed
439 delay time in the light-on response, but by the response to a light-off stimulus (Fig. 6, 7).
440 While several previous models have been presented to explain the photobehavior of

441 green alga, ours is one of the simplest, explaining the switching of the phototactic sign
442 through only one equation with some changes of the system parameters (Bennett &
443 Golestanian, 2015; Drescher et al., 2010).

444 Our model also provides clues to understanding why all the cells of the same
445 strain under the same light conditions do not exhibit the same sign of phototaxis; for
446 example, even when PP cells are treated with H_2O_2, which elicits positive phototaxis,
447 ~5% of the cells show negative phototaxis (Wakabayashi et al., 2011). This could be
448 explained by the variance of the delay time in the onset of ciliary dominance. Even
449 though our model precludes the fixed delay time after treatment with the
450 ROS-modulating reagents, the delay time may vary between cells. In Fig. 5, when γ_0 =
451 1 (i.e., the *trans*-cilium is dominant after photoreception) and I_0 = 0.1 or 0.5, cells show
452 positive phototaxis when ~50 < τ_0 < ~300 msec. The value of τ_0 has been suggested to
453 be longer than 30~40 msec (Rüffer & Nultsch, 1991; Witman, 1993). Thus, if a cell has
454 longer τ_0 than 300 msec, which would be caused by several factors including kinetics of
455 Ca^{2+} influx and cellular ROS amounts, this cell will exhibit negative phototaxis.
456 Furthermore, the τ_0-vz curves in Fig. 5 will change greatly if the eyespot position
457 somewhat varies and causes a change in the τ_0-vz curve. If a cell has the eyespot at an
458 irregular position, it may exhibit an opposite sign of phototaxis even with the same τ_0.

In summary, our experimental observations combined with the insights from our theoretical model showed that phototactic signs of *C. reinhardtii* cells are determined by two factors: the genetically determined dominant cilium, and the timing of the onset of strong beating by the dominant cilium after photoreception (Fig. 7). The timing, either on the light side or the dark side, is modulated by the cellular amount of ROS, which is a byproduct of photosynthesis. Cells may monitor photosynthetic activities through ROS amounts, and this regulation mechanism may contribute to maintaining ideal photosynthetic activities by modifying light conditions through phototaxis.

MATERIALS AND METHODS

Cell culture and strains

Chlamydomonas reinhardtii strains CC-124 (nit1− (nitrate reductase), nit2−, agg1−, mt− (mating type))(Ide et al., 2016), CC-125 (nit1−, nit2−, mt+), CC-2670 (ida4-, mt+), and CC-2228 (oda1-, mt+) were used. CC-124 and CC-125 were termed PP and NP, respectively. The CC-125 strain maintained in our laboratory appears to have a slight difference in motility characteristics from the same strain available from the Chlamydomonas Resource Center (http://www.chlamycollection.org/) (Sato, Sato, & Toyoshima, 2018; Wakabayashi et al., 2011). CC-2670 (*ida4*; lacking inner-arm dyneins a, c, and d) and CC-2228 (*oda1*; lacking outer-arm dynein and the outer-dynein arm docking complex) were used as slow-swimming mutants. Cells were grown in tris-acetate phosphate medium (TAP) medium with aeration at 25 °C, on a 12 h/12 h light/dark cycle (Gorman & Levine, 1965).

High-speed observation of phototaxis and measurement of the bodily rotation cycle

Cells were washed with an experimental solution (5 mM Hepes (pH 7.4), 0.2 mM EGTA, 1 mM KCl, 0.3 mM $CaCl_2$) (Okita, Isogai, Hirono, Kamiya, & Yoshimura, 2005) and kept under red light for more than 50 minutes before the assays. To induce

positive or negative phototaxis, the cell suspensions were treated with tertiary-butylhydroperoxide (*t*-BOOH; final concentration is 0.2 mM) (Wako Pure Chemical Industries) as a ROS reagent, or dimethylthiourea (DMTU; final concentration is 75 mM) (Sigma-Aldrich) as a ROS-scavenging reagent (Wakabayashi et al., 2011). Cell suspensions were put between a coverslip and a glass slide and placed on the stage of a dark-field microscope with an oil-immersion condenser (BX53; Olympus). The directional light to induce phototaxis was produced with two green LEDs (λ=525 nm). The setup is shown in Fig. 2A. First, a weak green light (~5 μmol photons m^{-2} s^{-1}) was illuminated (Light 1 in Fig. 2A). Most cells showed either positive or negative phototaxis. Then a stronger green light (Light 2 in Fig. 2A; ~30 μmol photons m^{-2} s^{-1}) was illuminated, perpendicular to Light 1. Most of the cells then changed their swimming directions and oriented parallel to the Light 2 beam. The behavior of cells was observed with dim red light (λ >600 nm) and videos were recorded with a high-speed camera (HAS-L2M, DITECT) at 150 fps. The LED for Light 2 was linked with the trigger switch of the high-speed camera so that recording was initiated when it was lit. The timing of photoreception was determined as the time when the eyespot faced the Light 2 side (Fig. 2A, 2B). The position of the eyespot in the helical swimming paths was also determined from the same video footage.

505 The measurement of the bodily rotation cycle was carried out with the same
506 experimental setup as above (without sideways illuminations). The time required for
507 one bodily rotation was determined from the position of the eyespot on the swimming
508 trajectories, and the rotation period was calculated.
509
510 ***Phototaxis assay***
511 The phototaxis assay shown in Fig. 5 was carried out by the method described in (Ueki
512 et al., 2016). In brief, cells were washed with the experimental solution and kept under
513 dim red light for 30 min before the phototaxis assays. For dish assays, cell suspensions
514 ($\sim 10^7$ cells/mL) were put in Petri dishes (30 mm in diameter, 10 mm thick), illuminated
515 with a green LED (λ =525 nm, ~50 μmol photons m^{-2} s^{-1}) from one side for 5 min, and
516 photographed (DSC-RX100M2; Sony). For single-cell analysis, cells were observed
517 under a dark-field microscope (BX-53, Olympus) under dim red light (λ > 600 nm) and
518 recorded to video using a CCD camera (1129HMN1/3; Wraymer). The angle (θ)
519 between the light direction and the swimming direction was measured for 1.5 s,
520 following illumination with a green LED for 15 s. Images of swimming cells were
521 auto-tracked using Image Hyper software (Science Eye), and angles were measured
522 from the cell trajectories. t-BOOH (final concentration of 0.2 mM; Wako Pure

Chemical Industries) was used as a ROS reagent, and dimethylthiourea (final concentration of 75 mM; Sigma-Aldrich) was used as a ROS-scavenging reagent

Electrophysiology

PRCs were assessed in a population of *C. reinhardtii* cells by the method of Sineshchekov et al. (1992) (O. A. Sineshchekov et al., 1992, 1994). In brief, 1 ml of cell suspension in a measuring solution (0.5 mM Hepes, pH 7.3, 0.1 mM $CaCl_2$) was put in a cuvette (10×10×15 mm), with two electrodes on each side of its rectangular bottom. A 500 nm beam of light was generated with an LED source (NSPE510S, Nichia Chemical) and applied from one side of the electrode. The current was measured with a patch-clamp amplifier (Axoclamp 200B, Axon).

Measurement of ciliary beating frequency

Ciliary beating frequency (CBF) was measured based on the method described in (R Kamiya, 2000) with modifications (Wakabayashi & King, 2006). The median frequency was obtained from the power spectra of fast Fourier-transformed cell body vibration signals in microscopy images averaged for ~20 s.

541 ***Measurement of bodily rotation cycle***

542 Cells were observed under a dark-field microscope with an oil-immersion condenser

543 (BX-53, Olympus) and recorded to video with a high-speed camera (HAS-L2M,

544 DITECT) at 150 fps. The bodily rotation cycle was defined as the time it takes for the

545 eyespot (observed as a bright spot) to return to the same position relative to the cell's

546 swimming trajectory, and was measured by counting the frames for one cycle.

547

548

549

Acknowledgments

This work was supported by Japan Society for the Promotion of Science KAKENHI Grants 19H03242 to KW, 16H06556 to TH, 17H02939 to KS, 17K07370 to KY, 19K23758 to NU, by Ohsumi Frontier Science Foundation to KW, by Global Station for Soft Matter at Hokkaido University to KS and TN, by Dynamic Alliance for Open Innovation Bridging Human, Environment and Materials to TH, KS, TN, and KW and by the Japan Agency for Medical Research and Development (AMED/PRIME) grant JP18gm5810013 to KY.

Competing interests

The authors declare that no competing interests exist.

562 **References**

563 Bennett, R. R., & Golestanian, R. (2015). A steering mechanism for phototaxis in
564 Chlamydomonas. *J R Soc Interface, 12*(104), 20141164.
565 Bohm, M., Boness, D., Fantisch, E., Erhard, H., Frauenholz, J., Kowalzyk, Z., . . .
566 Kreimer, G. (2019). Channelrhodopsin-1 Phosphorylation Changes with
567 Phototactic Behavior and Responds to Physiological Stimuli in Chlamydomonas.
568 *Plant Cell, 31*(4), 886-910.
569 Drescher, K., Goldstein, R. E., & Tuval, I. (2010). Fidelity of adaptive phototaxis. *Proc*
570 *Natl Acad Sci U S A, 107*(25), 11171-11176.
571 Feinleib, M. E. H., & Curry, G. M. (1971). The relationship between stimulus intensity
572 and oriented phototactic response (topotaxis) in Chlamydomonas. In
573 *Physiologia Plantarum* (Vol. 25, pp. 346-352).
574 Foster, K. W., & Smyth, R. D. (1980). Light Antennas in phototactic algae. *Microbiol*
575 *Rev, 44*(4), 572-630.
576 Gorman, D. S., & Levine, R. P. (1965). Cytochrome f and plastocyanin: their sequence
577 in the photosynthetic electron transport chain of Chlamydomonas reinhardi.
578 *Proc Natl Acad Sci U S A, 54*(6), 1665-1669.
579 Ide, T., Mochiji, S., Ueki, N., Yamaguchi, K., Shigenobu, S., Hirono, M., &
580 Wakabayashi, K.-i. (2016). Identification of the agg1 mutation responsible for
581 negative phototaxis in a “wild-type” strain of Chlamydomonas reinhardtii.
582 *Biochemistry and Biophysics Reports, 7*, 379-385.
583 Iomini, C., Li, L., Mo, W., Dutcher, S. K., & Piperno, G. (2006). Two flagellar genes,
584 AGG2 and AGG3, mediate orientation to light in Chlamydomonas. *Curr Biol,*
585 *16*(11), 1147-1153.
586 Isogai, N., Kamiya, R., & Yoshimura, K. (2000). Dominance between the two flagella
587 during phototactic turning in Chlamydomonas. *Zool Sci, 17*, 1261-1266.
588 Kamiya, R. (1988). Mutations at twelve independent loci result in absence of outer
589 dynein arms in Chlamydomonas reinhardtii. *J Cell Biol, 107*(6 Pt 1), 2253-2258.
590 Kamiya, R. (2000). Analysis of cell vibration for assessing axonemal motility in
591 Chlamydomonas. *Methods, 22*, 383-387.
592 Kamiya, R., & Hasegawa, E. (1987). Intrinsic difference in beat frequency between the
593 two flagella of Chlamydomonas reinhardtii. *Exptl. Cell Res., 173, 299-304*.
594 Kamiya, R., Kurimoto, E., & Muto, E. (1991). Two types of Chlamydomonas flagellar
595 mutants missing different components of inner-arm dynein. *J Cell Biol, 112*(3),
596 441-447.

597 Kamiya, R., & Witman, G. B. (1984). Submicromolar levels of calcium control the
598 balance of beating between the two flagella in demembranated models of
599 Chlamydomonas. *J Cell Biol, 98*(1), 97-107.
600 Kondo, T., Johnson, C. H., & Hastings, J. W. (1991). Action spectrum for resetting the
601 circadian phototaxis rhythm in the CW15 strain of Chlamydomonas 1. Cells in
602 darkness. *Plant Physiol, 95*, 197-205.
603 Landau, L. D., Lifshitz, E. M. (1976). *Mechanics, 3rd ed.* (Vol. 1 (Course of Theoretical
604 Physics)): Oxford: Butterworth- Heinemann.
605 Morel-Laurens, N. (1987). Calcium control of phototactic orientation in
606 Chlamydomonas reinhardtii: sign and strength of response. *Photochem*
607 *Photobiol, 45*(1), 119-128.
608 Nagel, G., Ollig, D., Fuhrmann, M., Kateriya, S., Musti, A. M., Bamberg, E., &
609 Hegemann, P. (2002). Channelrhodopsin-1: a light-gated proton channel in green
610 algae. *Science, 296*(5577), 2395-2398.
611 Nagel, G., Szellas, T., Huhn, W., Kateriya, S., Adeishvili, N., Berthold, P., . . . Bamberg,
612 E. (2003). Channelrhodopsin-2, a directly light-gated cation-selective membrane
613 channel. *Proc Natl Acad Sci U S A, 100*(24), 13940-13945.
614 Okita, N., Isogai, N., Hirono, M., Kamiya, R., & Yoshimura, K. (2005). Phototactic
615 activity in Chlamydomonas 'non-phototactic' mutants deficient in
616 Ca2+-dependent control of flagellar dominance or in inner-arm dynein. *J Cell*
617 *Sci, 118*(Pt 3), 529-537.
618 Ruffer, U., & Nultsch, W. (1987). Comparison of the beating of cis- and trans-flagella of
619 Chlamydomonas cells held on micropipettes. *Cell Motil Cytoskeleton, 7*, 87-93.
620 Ruffer, U., & Nultsch, W. (1998). Flagellar coordination in Chlamydomonas cells held
621 on micropipettes. *Cell Motil Cytoskeleton, 41*(4), 297-307.
622 Rüffer, U., & Nultsch, W. (1991). Flagellar photoresponses of Chlamydomonas cells
623 held on micropipettes: II. Change in flagellar beat pattern. *Cell Motility*
624 *Cytoskeleton, 18*(4), 269-278.
625 Sato, N., Sato, K., & Toyoshima, M. (2018). Analysis and modeling of the inverted
626 bioconvection in Chlamydomonas reinhardtii: emergence of plumes from the
627 layer of accumulated cells. *Heliyon, 4*(3), e00586.
628 Sineshchekov, O. A., Govorunova, E. G., Der, A., Keszthelyi, L., & Nultsch, W. (1992).
629 Photoelectric Responses in Phototactic Flagellated Algae Measured in
630 Cell-Suspension. *J Photochem Photobiol B-Biology, 13*(2), 119-134.
631 Sineshchekov, O. A., Govorunova, E. G., Der, A., Keszthelyi, L., & Nultsch, W. (1994).
632 Photoinduced electric currents in carotenoid-deficient Chlamydomonas mutants

633 reconstituted with retinal and its analogs. *Biophys J, 66*(6), 2073-2084.
634 Sineshchekov, O. A., Jung, K.-H., & Spudich, J. L. (2002). Two rhodopsins mediate
635 phototaxis to low- and high-intensity light in Chlamydomonasreinhardtii. *PNAS, 99*(13), 8689-8694.
636
637 Suzuki, T., Yamasaki, K., Fujita, S., Oda, K., Iseki, M., Yoshida, K., . . . Takahashi, T.
638 (2003). Archaeal-type rhodopsins in Chlamydomonas: model structure and
639 intracellular localization. *Biochem Biophys Res Commun, 301*(3), 711-717.
640 Takada, S., Wilkerson, C. G., Wakabayashi, K., Kamiya, R., & Witman, G. B. (2002).
641 The outer Dynein arm-docking complex: composition and characterization of a
642 subunit (oda1) necessary for outer arm assembly. *Mol Biol Cell, 13*(3),
643 1015-1029.
644 Takahashi, T., & Watanabe, M. (1993). Photosynthesis modulates the sign of phototaxis
645 of wild-type Chlamydomonas reinhardtii. Effects of red background illumination
646 and 3-(3',4'-dichlorophenyl)-1,1-dimethylurea. *FEBS Lett, 336*(3), 516-520.
647 Ueki, N., Ide, T., Mochiji, S., Kobayashi, Y., Tokutsu, R., Ohnishi, N., . . . Wakabayashi,
648 K. (2016). Eyespot-dependent determination of the phototactic sign in
649 Chlamydomonas reinhardtii. *Proc Natl Acad Sci U S A, 113*(19), 5299-5304.
650 Vergara, C., Latorre, R., Marrion, N. V., & Adelman, J. P. (1998). Calcium-activated
651 potassium channels. *Curr Opin Neurobiol, 8*(3), 321-329.
652 Wakabayashi, K., & King, S. M. (2006). Modulation of Chlamydomonas reinhardtii
653 flagellar motility by redox poise. *J Cell Biol, 173*(5), 743-754.
654 Wakabayashi, K., Misawa, Y., Mochiji, S., & Kamiya, R. (2011). Reduction-oxidation
655 poise regulates the sign of phototaxis in Chlamydomonas reinhardtii. *Proc Natl*
656 *Acad Sci U S A, 108*(27), 11280-11284.
657 Witman, G. B. (1993). Chlamydomonas phototaxis. *Trends Cell Biol, 3*, 403-408.

658

659 **Table 1. Ciliary beating frequencies and bodily rotation cycles of strains used**

	PP	NP	*ida4*	*oda1*
Ciliary Beating Frequency (Hz) (Mean ± SEM, n=3 measurements)	55.0 ± 0.6	55.5 ± 1.0	51.6 ± 2.6	24.3 ± 0.6
Bodily rotation cycle (Hz) (Mean ± SD, n=10 cells)	2.11 ± 0.27	1.89 ± 0.27	1.25 ± 0.22	0.72 ± 0.09

660

661

Figure legends

Fig. 1

Schematic images of a *Chlamydomonas reinhardtii* cell and its phototaxis.

(A) Schematic image of *C. reinhardtii* cell and the eyespot. The cilium closest to the eyespot is called *cis*-cilium, whereas the one farthest from the eyespot is called *trans*-cilium. The eyespot is composed of the carotenoid-rich granule layers that function as a light reflector, and channelrhodopsin molecules aligned in the plasma membrane. Channelrhodopsin functions as a light-gated cation channel. The light signal coming from the outside of the cell is reflected by the carotenoid granule layers and amplified, whereas that coming through the cell is blocked. (B) The current model to explain positive phototaxis. After photoreception at the eyespot (yellow arrow), $[Ca^{2+}]_i$ in the cilia increases and the *trans*-cilium (t) becomes dominant. After a half rotation of the cell around its central axis, the light signal to the eyespot is blocked, $[Ca^{2+}]_i$ in the cilia decreases, and the *cis*-cilium (c) becomes dominant. (C) Hypothetical models for negative phototaxis. In the “Dominant arm model”, Ca^{2+}-sensitivities of two cilia are assumed to be reversed from the positively phototactic cell shown in (B); the *cis*-cilium becomes dominant after photoreception. In the “Off-response model”, after

679 photoreception, the *trans*-cilium becomes dominant when the eyespot faces opposite to
680 the light source.
681
682 **Fig. 2**
683 **Eyespot position relative to the cell trajectory during phototaxis.**
684 **(A)** Phototactic turnings of PP and NP cells after treatment with t-BOOH or DMTU.
685 Images of a swimming cell, taken at 150 fps, are superimposed every 0.13 sec. First,
686 Light 1 (weak green light from the left) was illuminated to induce positive (top;
687 swimming to the left) or negative (bottom; swimming to the right) phototaxis. After
688 Light 2 (strong green light from the top) was turned on, the cell changed its swimming
689 direction. The timing of the onset of Light 2 was at the white arrows/arrowhead. The
690 eyespot facing Light 2 is shown with green arrowheads, whereas that facing opposite to
691 Light 2 is shown with magenta arrowheads. The former case is classified as “the light
692 side”) and the latter “the dark side” in **(B).** Yellow arrows show the swimming
693 directions. (The cells whose trajectories intersect with the superimposed cells were
694 removed from the image in the process creating the superimpose. See SI Movies S1-4
695 for the raw data.) **(B)** The proportion of the dominant cilium and the side where the
696 onset of the ciliary dominance occurred. PP cells showing positive phototaxis (control

and +*t*-BOOH) or negative phototaxis (+DMTU) and NP cells showing negative phototaxis (control and +DMTU) or positive phototaxis (+*t*-BOOH) were observed (n=8~28 per condition).

Fig. 3

Mathematical model for *C. reinhardtii* phototaxis.

(A) Definitions of the body axes of a *C. reinhardtii* cell. The vectors **a**, **b** and **c** are unit vectors that are fixed to the body of the cell. **a**, **b** and **c** are mutually orthogonal to each other, and **b** and **c** are within the ciliary beat plane. **b** is close to the side of *cis*-cilium. With them, the direction of eyespot is expressed as $\mathbf{e}_{eyespot} = (\mathbf{b}+\mathbf{c})/\sqrt{2}$. The directions of **a**, **b** and **c** evolve with time according to Eq. 1. **(B)** Definitions of the Euler angles that specify the directions of **a**, **b**, **c** for the x, y, z coordinate system that is fixed in space. θ_1 is the angle between the y-axis and the vector $\mathbf{N}$, where $\mathbf{N} = \mathbf{z}\times\mathbf{c}/|\mathbf{z}\times\mathbf{c}|$. θ_2 and θ_3 are angles between the z-axis and $\mathbf{c}$ and between $\mathbf{N}$ and $\mathbf{b}$, respectively. When $\theta_1 = \theta_2 = \theta_3 = 0$, **a**, **b**, **c** axes coincide with x, y, z axes, respectively. **(C), (D)** Examples of initial trajectories of the cell obeying Eq. 1 ($0 \le t \le 10$), which indicate positive phototaxis (τ_0 =0.08 sec, **(C)**) and negative phototaxis (τ_0 =0.32 sec. **(D)**). The parameters are $\gamma_0 = 1$ (the *trans*-cilium becomes

715 dominant after photoreception at the eyespot) and $I_0 = 0.5$, and the initial conditions

716 are $\mathbf{r}(0) = (0,0,0)$, $\theta_1(0) = 0$, $\theta_2(0) = -\pi/2$ and $\theta_3(0) = 0$. Thick orange arrows

717 show the direction of the light illumination, and thin black arrows show the swimming

718 direction of the cell.

719

720 **Fig. 4**

721 **Sign-switching of phototaxis in the mathematical model.**

722 The mean velocity $\bar{v}_z$ of the steady-state of the cell after a long-time simulation as a

723 function of the delay time τ_0 for various values of γ_0 and I_0. For each set of system

724 parameters, only one steady state of Eq. 1 realizes, which does not depend on the initial

725 conditions of θ_1, θ_2, θ_3, $\mathbf{r}$. $\bar{v}_z$ changes with τ_0; especially, the sign of $\bar{v}_z$ (=the

726 sign of phototaxis) changes with γ_0 and τ_0. Blue dots are the states where solution S5

727 realizes, while red dots are the states where solution S6 realizes. Black dots with bars

728 are the states where solutions other than Eqs. S5 or S6 are achieved, in which $v_z(t)$

729 oscillates in time. The bars indicate the standard deviation of v_z of the steady-state.

730 The parameter values used are $v_0 = 120$ [μm/s], [1/s] and $\omega_a^{(0)} = 2\pi$ [1/s]. The initial

731 conditions are: $\mathbf{r}(0) = (0,0,0)$, $\theta_i(0) = \delta_i$ with random numbers $\delta_i \in [0, 2\pi]$ for

732 $i = 1,2,3$, and $dI(t)/dt = 0$ for $0 \le t \le \tau_0$. For the discretization of Eq. S1, the Euler

733 method was used ($\Delta t = 1/10000$). The model suggests that, when γ_0=1 (i.e. the

734 *trans*-cilium is dominant), the cell shows positive phototaxis (i.e. γ_0 is positive) when

735 the dominant cilium beats stronger than the *cis*-cilium with the delay (τ_0) 50~260 ms.

736 Similarly, when γ_0=-1 (i.e. the *cis*-cilium is dominant), the cell shows negative

737 phototaxis under the same conditions.

738

739 **Fig. 5**

740 **Phototaxis assay of the slow-swimming mutants.**

741 **(A)** PP, NP, *oda1*, and *ida4* cell suspensions put in Petri dishes with or without

742 ROS-modulating reagents (0.2 mM *t*-BOOH or 75 mM DMTU) were illuminated by

743 green LED (λ=525 nm, 30 μmol photons m^{-2} s^{-1}) from the right (green arrows) for 5 min

744 from the right. Cells showing positive phototaxis are accumulated in the right halves of

745 the dishes (orange boxes with "P") and those showing negative phototaxis are

746 accumulated in the left halves of the dishes (blue boxes with "N"). **(B)** Polar histograms

747 depicting the percentage of cells moving in a particular direction relative to light

748 illuminated from the right (green arrows), with or without treatment with

749 ROS-modulating reagents (12 bins of 30°; n = 30 cells per condition).

750

Fig. 6

Sign-switching of phototaxis in a slow-swimming mutant in the mathematical model.

The plot of the mean velocity $\bar{v}_z$ of the steady-state of the mathematical model (Eqs. S3 and S4) concerning the delay time τ_0 for cells rotate at 0.67 Hz, three times slower than typical wild-type cells (~2.0 Hz). The parameter values used here are the same as those used in Fig. 4 except for $\omega_\alpha^{(0)}$ representing the bodily rotation cycle. The meanings of blue, red, and black dots and bars in this figure are the same as those in Fig. 4.

Fig. 7

Schematic model of sign-reversal in phototaxis suggested by this study.

To make a phototactic turning, *cis*-dominant strain beats the *cis*-cilium (C) stronger than the *trans*-cilium (T), whereas *trans*-dominant strain beats the *trans*-cilium stronger than the *cis*-cilium. The *trans*-dominant strain, such as PP in this study, shows positive phototaxis when the strong beating occurs upon light-on response (i.e. when the eyespot faces the light side) and negative phototaxis when it occurs upon light-off response (i.e. when the eyespot faces the dark side). The *cis*-dominant strain, such as NP in this study,

769 shows negative phototaxis when the strong beating occurs upon light-on response and

770 positive phototaxis when it occurs light-off response.

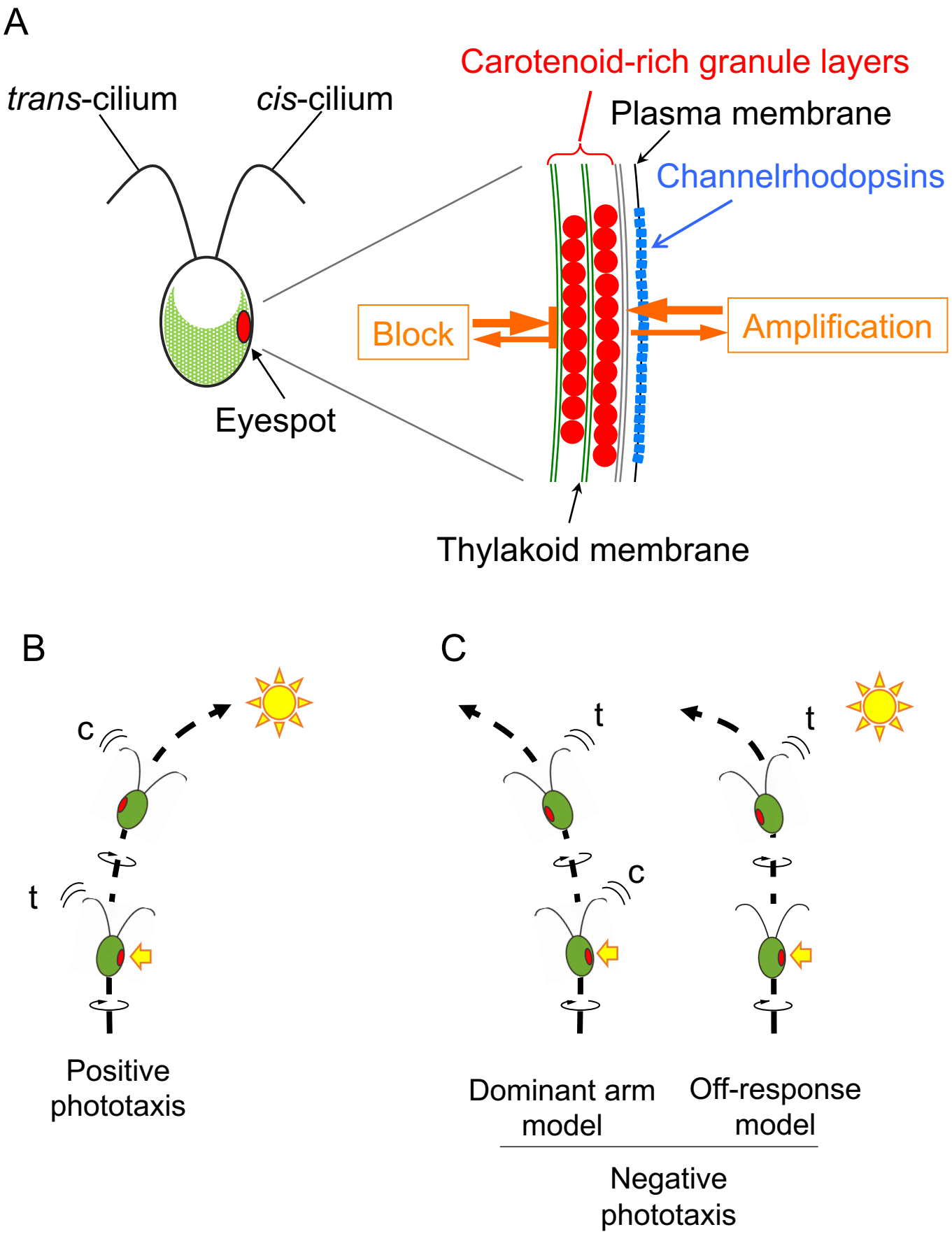

Fig. 1 **Schematic images of a *Chlamydomonas reinhardtii* cell and its phototaxis.**

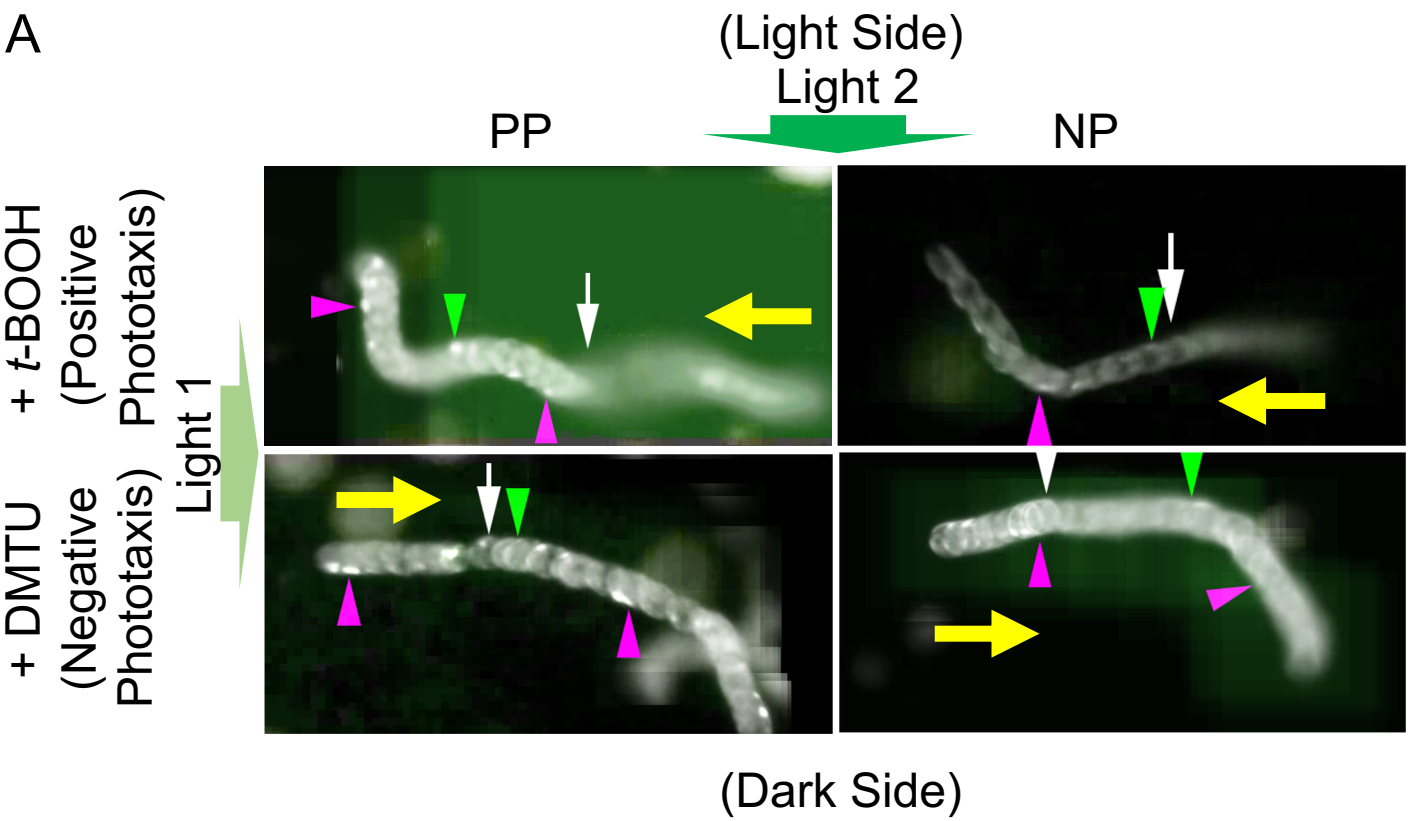

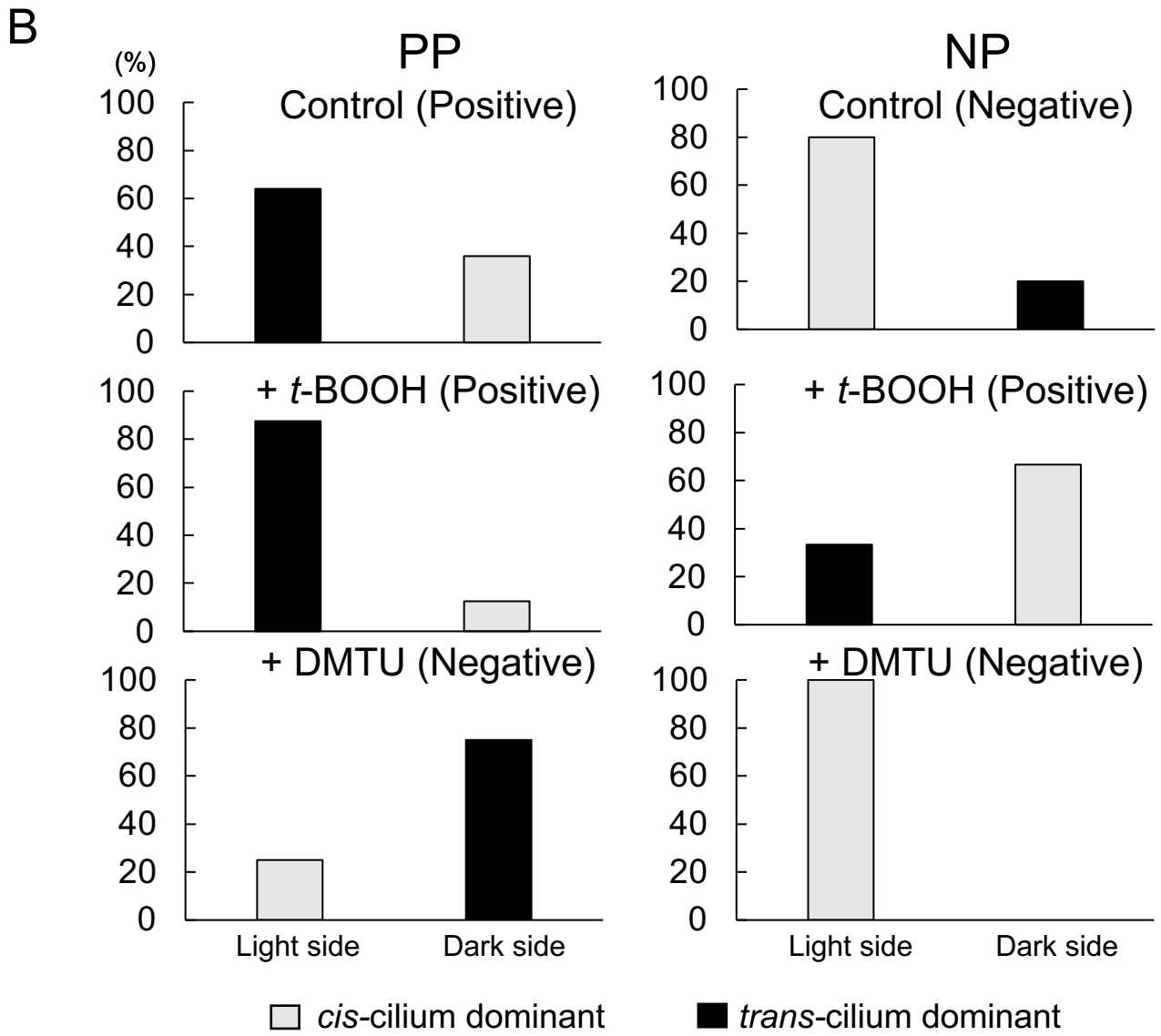

Fig. 2 **Eyespot position relative to the cell trajectory during phototaxis.**

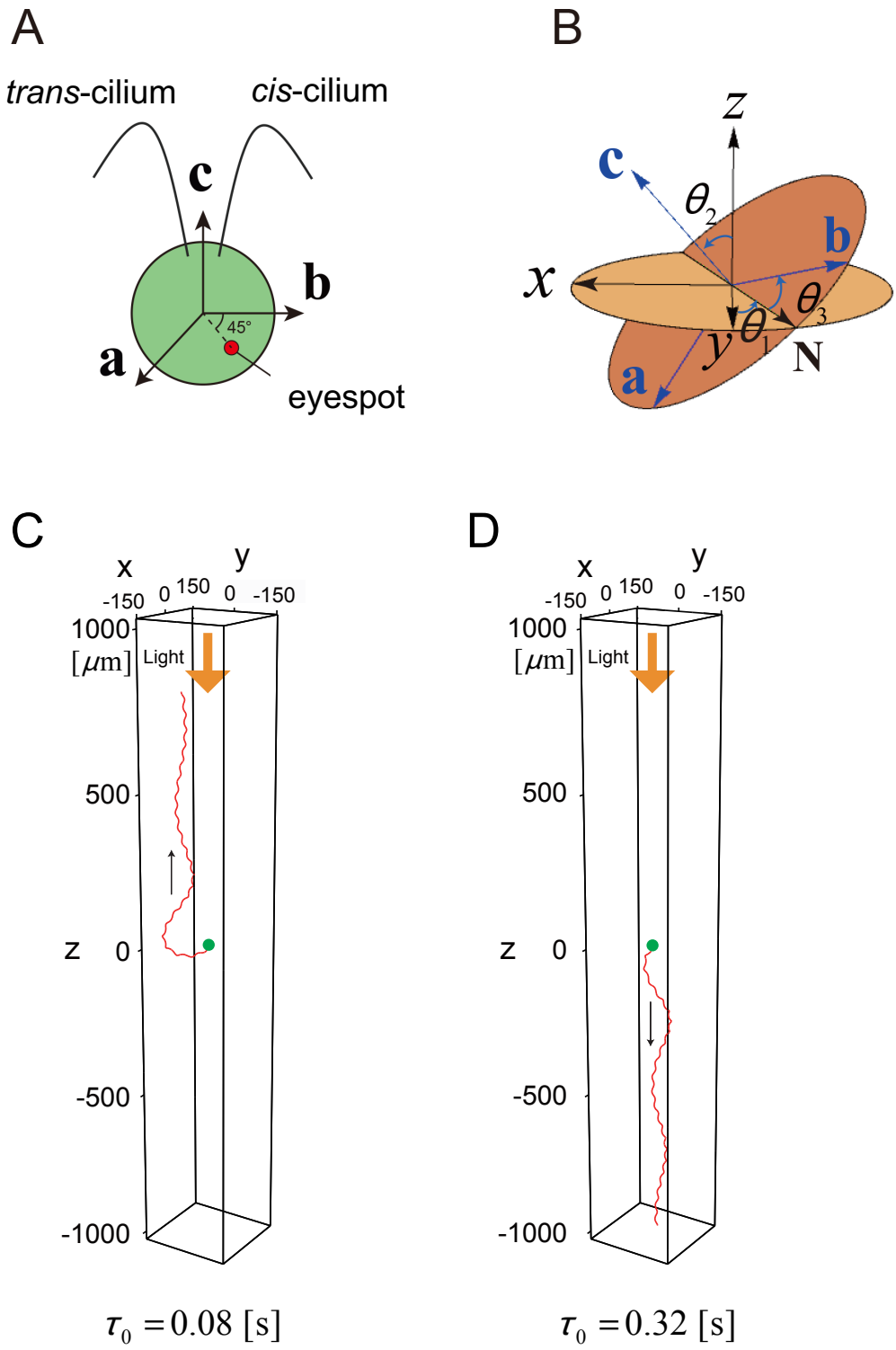

Fig. 3 **Mathematical model for *C. reinhardtii* phototaxis.**

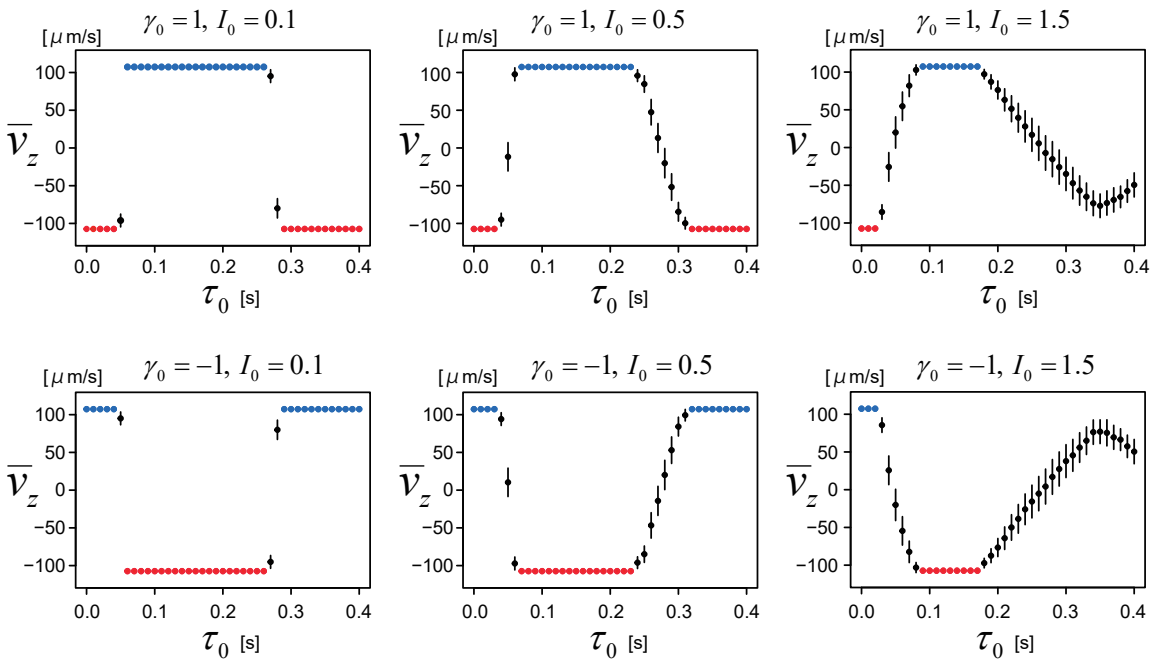

Fig. 4 **Sign-switching of phototaxis in the mathematical model.**

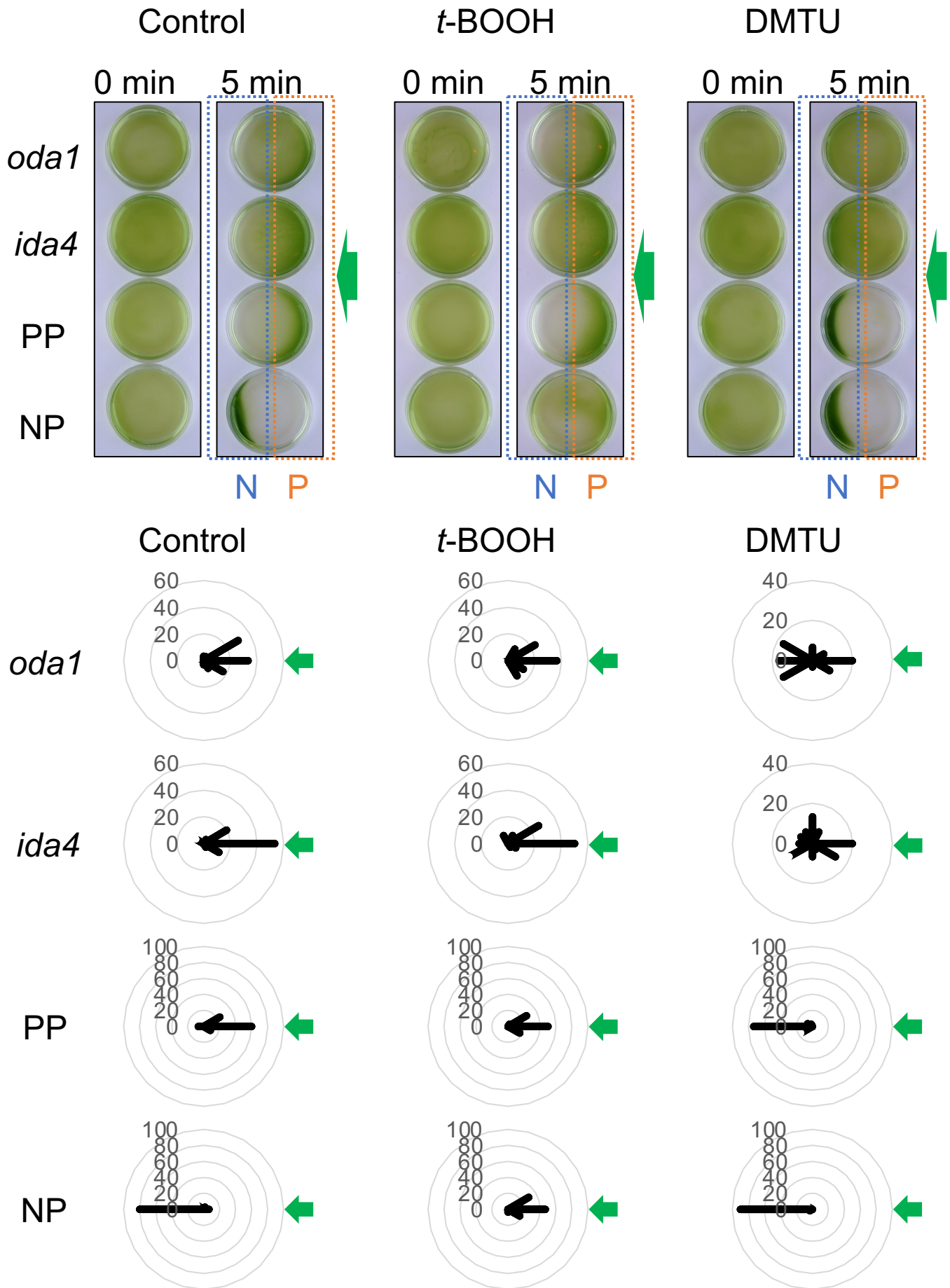

Fig. 5 **Phototaxis assay of the slow-swimming mutants.**

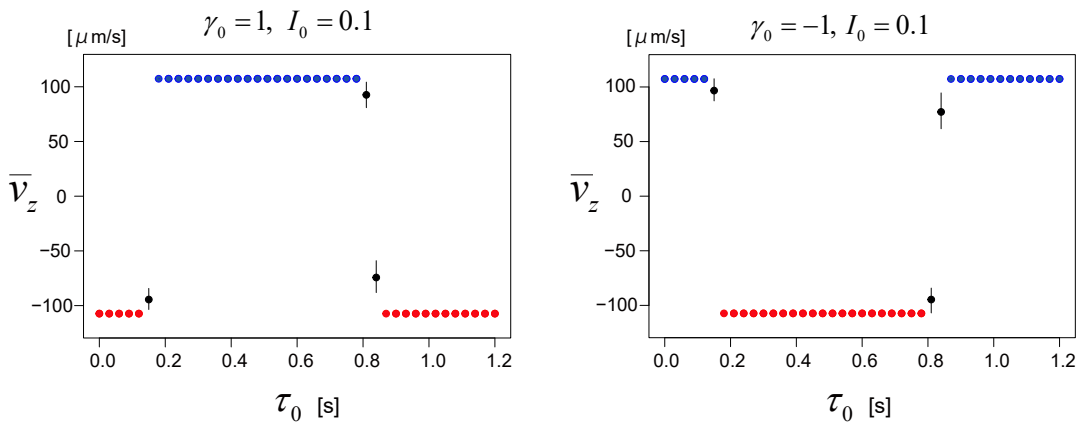

Fig. 6 **Sign-switching of phototaxis in a slow-swimming mutant in the mathematical model.**

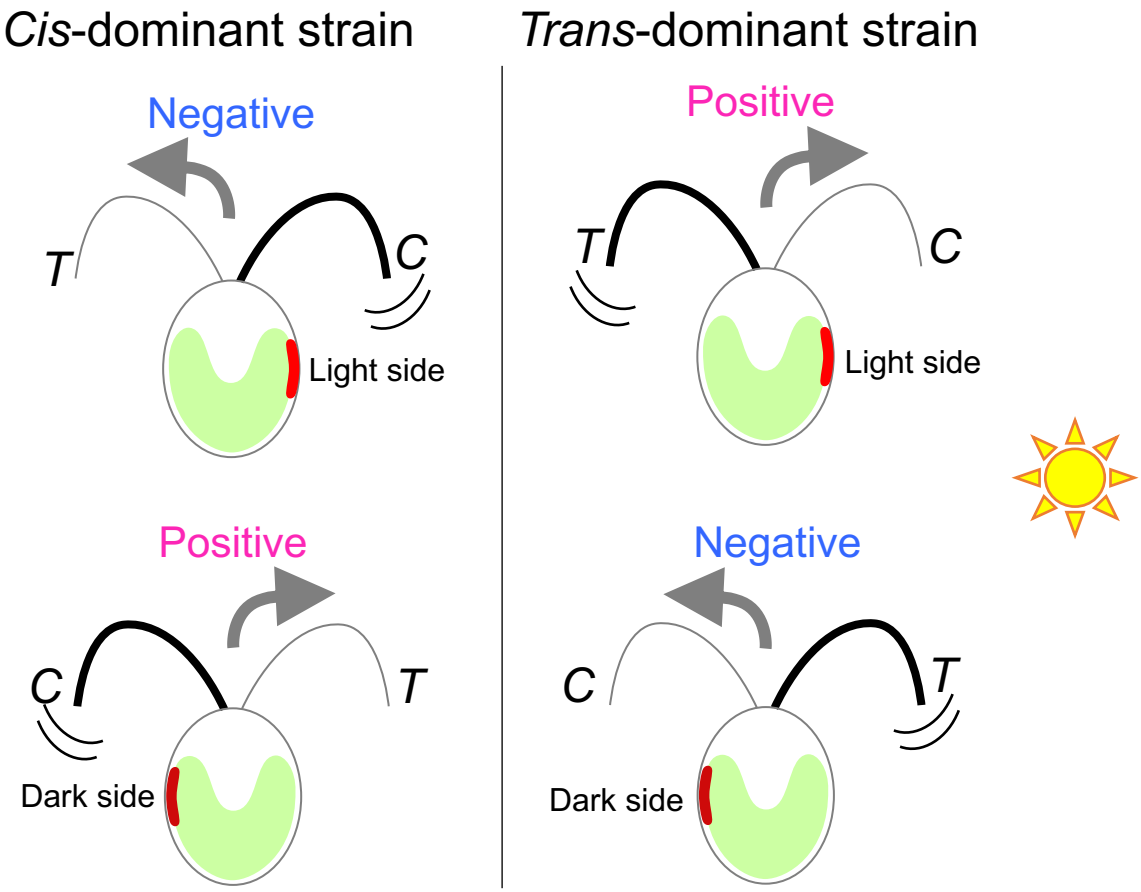

Fig. 7 **Schematic model of sign-reversal in phototaxis suggested by this study.**